

# Photoproduction of Mesons off Nuclei - The Photonuclear Programs at ELSA and MAMI

**B. Krusche**

Department of Physics, University of Basel, CH-4056 Basel, Switzerland  
for the CBELSA/TAPS and Crystal Barrel/TAPS collaborations

E-mail: [Bernd.Krusche@unibas.ch](mailto:Bernd.Krusche@unibas.ch)

**Abstract.** Recent results for the photoproduction of mesons from nuclei with tagged bremsstrahlung beams are summarized. The experiments have been done at the Mainz MAMI accelerator with the Crystal Ball/TAPS setup and at the Bonn ELSA accelerator with the Crystal Barrel/TAPS detector. Two main physics topics are covered. The electromagnetic excitation spectrum of the neutron has been studied with meson photoproduction reactions off quasi-free neutrons from light nuclei. Particularly interesting results have been obtained for  $\eta$ -photoproduction, where the excitation function of the neutron shows a pronounced, narrow structure which is not observed for the proton. The interaction of mesons with nuclear matter and the in-medium properties of hadrons under various aspects have been studied with meson photoproduction from nuclei, covering a large mass range (from the deuteron to lead). Questions like the possible formation of  $\eta$ -mesic nuclei and in-medium modifications of the  $\sigma$ -meson have been addressed.

## 1. Introduction

Photoproduction of mesons off nuclei is important for two different lines of research. The electromagnetic excitation spectrum of the neutron can only be studied in quasi-free kinematics with neutrons bound in light nuclei, in particular in the deuteron. Photoproduction of mesons from heavy nuclei is a very useful tool for the study of meson - nucleus interactions, or more generally the study of hadron-in-medium properties. Both lines of research form a significant part of the research programs at the Bonn ELSA and Mainz MAMI tagged photon facilities.

### *1.1. Quasi-free photoproduction off the neutron*

In the same way in which the excitation spectra of atoms reflect the properties of the electromagnetic interaction, and the level schemes of nuclei reveal many details about the interaction between nucleons, are the excited states of the nucleon related to the fundamental properties of the strong interaction. Quantum Chromodynamics (QCD) at this energy scale is non-perturbative so that so far the experimental results could only be interpreted by phenomenological quark models. These models are based on different internal degrees of freedom (three equivalent constituent quarks, quark-diquark structures, additional collective modes) and different residual interactions of the quarks (gluon exchange, Goldstone boson exchange). Although it is evident, that such models can only serve as an approximation of the complicated structure of the nucleon, the idea was of course that a comparison of the observed excitation spectrum to the model results should at least give some guidance concerning the

relevant properties of the interaction. However, so far this approach had only limited success. The confrontation of model results with data indicates similar problems for all models and no particular models can be clearly preferred. Already the positioning of some of the lowest lying, and therefore most basic, excited states is notoriously problematic. The  $N(1440)P_{11}$  ('Roper') and the  $\Delta(1600)P_{33}$  states, which in the quark models both belong to the  $N=2$  oscillator band, appear in nature well below the states assigned to the  $N=1$  band. At higher excitation energies not only the ordering but already the match in simple number counting is poor; many more states are predicted than have been observed. Actually, with very few exceptions, for most combination of quantum numbers experimentally only the lowest lying state is known, while models predict a plethora of higher lying states. This problem became even more severe after the most recent partial-wave analysis of elastic pion scattering data by Arndt and collaborators [1] discarded almost half of the states listed in the Review of Particle Physics [2] as being due to statistical noise in earlier analyzes. However, here one must consider that also experimental bias could be at the center of the problem. Data analyses like the one cited above rely entirely on pion scattering and will therefore miss states that couple only weakly to  $\pi N$ . Since the higher the excitation energy the more decay channels are open and since there are quite some examples where nature prefers to invest in mass rather than in energy, it is not inconceivable that the higher lying states couple preferentially to decay channels involving heavier mesons or sequential decays via intermediate excited states.

Therefore, the still unanswered basic question is, whether this mismatch between experiment and model predictions is rooted in inappropriate internal degrees of freedom in the models or in bias in the experiments. Interestingly, first unquenched lattice results, which became available very recently [3], basically 're-discovered' the well-known  $SU(6)\otimes O(3)$  excitation structure of the nucleon and have a level counting consistent with the standard non-relativistic quark model, making simple arguments like a reduction of the effective number of degrees of freedom, e.g. by the formation of quark-diquark structures, less plausible. However, one should keep in mind, that these calculations are in a very early stage, still far away from the quality reached in the meantime for ground state properties of hadrons [4].

On the experimental side, during the last two decades photoproduction of mesons has developed into the prime tool for the experimental investigation of the excitation spectrum of the nucleon. It has now almost completely replaced meson induced reactions like elastic pion scattering. This development became possible due to the large progress in accelerator and detector technology, which nowadays allows to measure the photon induced reactions with at least comparable accuracy as hadron induced reactions, although the latter usually profit from production cross section which are larger by roughly three orders of magnitude. The choice of a different initial state and the investigation of many different final states avoid the bias against resonances that couple only weakly to  $N\pi$  and the exploration of multiple meson production reactions like  $\pi\pi$ ,  $\pi\eta$ ... is supposed to give access to resonances that decay mainly via intermediate excited states. Furthermore, photon induced reactions have the additional advantage that the electromagnetic couplings are related to the spin-flavor correlations of the states and thus carry information about configuration mixing, which is sensitive to the details of the model wave functions.

The measurement of photoproduction reactions off the free proton has made tremendous progress during the last few years and now approaches its final phase with the measurement of single and double polarization observables. However, the electromagnetic excitations are isospin dependent, so that also measurements of meson-production reactions off the neutron are required. Already the most simple observable, the total photoabsorption cross section, shows clearly different structures for the proton and neutron (see Fig. 1), demonstrating the expected differences in the electromagnetic excitation strengths. It is therefore possible, that resonances which couple (electromagnetically) only weakly to the proton may be more easily observed with

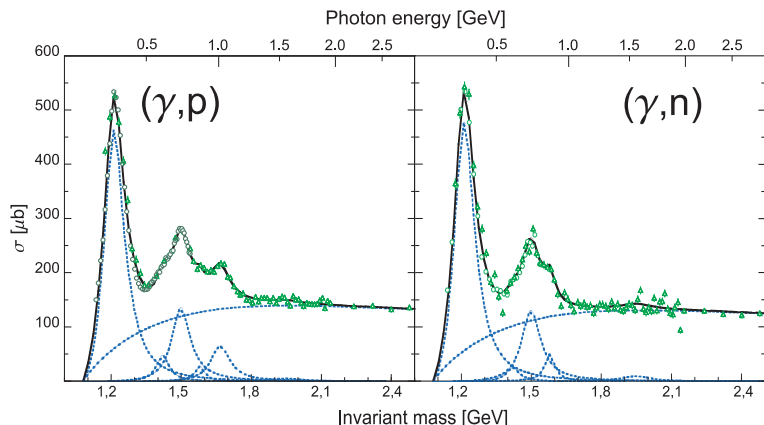


**Figure 1.** Cross section for total photoabsorption on the proton (left hand side) and the neutron (right hand side) [5]. Points: measured data, curves: fit of Breit-Wigner shapes of nucleon resonances ( $P_{33}(1232)$ ,  $P_{11}(1440)$ ,  $D_{13}(1520)$ ,  $S_{11}(1535)$ ,  $F_{15}(1680)$  (only for proton), and  $F_{37}(1950)$ ) and a smoothly varying background.

a neutron target. However, so far only few meson production reactions off the neutron have been measured, and most of them with much inferior quality than the corresponding reactions off the free proton. This is of course due to the complications related to the measurements off quasi-free neutrons bound in light nuclei. The detection of recoil neutrons, and even more the control of their detection efficiency, is non-trivial and the interpretation of the results is complicated by nuclear effects like Final State Interaction (FSI).

However, such programs have now been launched at CLAS, ELSA, and MAMI. These facilities are complementary because CLAS at Jlab is optimized for final states with charged particles, like e.g. from the  $\gamma n \rightarrow p\pi^-$  reaction, while the almost  $4\pi$ -covering electromagnetic calorimeters at ELSA and at MAMI can measure mixed charge and also complicated ‘all-neutral’ final states like  $n\pi^0\pi^0$ . We will discuss in this contribution recent results from ELSA and MAMI and pay special attention to the control of the systematic uncertainties in quasi-free production processes.

### 1.2. Meson photoproduction off heavier nuclei

Photoproduction of mesons from nuclei over a large range of mass numbers can be exploited for the investigation of meson-nucleus interactions, hadron-in-medium properties but also for less obvious topics like for example the study of nuclear mass form factors and nuclear matter transition form factors [6, 7, 8].

Elastic and inelastic reactions using secondary meson beams, in particular charged pions and kaons, have revealed many details of the nucleon - meson potentials. However, secondary meson beams are only available for long-lived, charged mesons. Much less is known for short-lived mesons like the  $\eta$ ,  $\eta'$ , and  $\omega$ . Their interactions with nuclei can be studied only in indirect ways. The general idea is to produce them by some initial reaction in a nucleus and then study their interaction with the same nucleus. The absorption properties of mesons in nuclear matter and the related in-medium life times (respectively widths) have been studied at ELSA and MAMI during the last few years for a couple of pseudoscalar mesons ( $\pi^0$  [9],  $\eta$  [10, 11],  $\eta'$  [12]) for the  $\omega$ -meson [13, 14, 15, 16] meson, and by the LEPS collaboration at SPring-8 also for  $\Phi$ -mesons [17], using the scaling of the cross sections with the atomic mass number  $A$ . The scaling is usually parameterized by

$$\frac{d\sigma}{dT}(T) \propto A^{\alpha(T)} \quad , \quad (1)$$

where  $T$  is the kinetic energy of the mesons. A value of  $\alpha$  close to unity corresponds to a cross section scaling with the volume of the nucleus, i.e. with vanishing absorption, while a value of  $\approx 2/3$  indicates surface proportionality, corresponding to strong absorption. These scaling coefficients can then be converted to absorption cross sections using for example Glauber-type approximation models. A basically equivalent concept are the so-called transparency ratios,

used in some of the above cited work, which compare the nuclear cross sections scaled by the nucleon number to the free nucleon cross section (or for practical reasons to the cross section of a light reference nucleus scaled by the mass number of that nucleus). An important result of such analyses is an in-medium width of the  $\omega$  meson on the order of 130 - 150 MeV in normally dense nuclear matter from which in a Glauber-type analysis, an absorption cross section of 70 mb was deduced [14]. This value is roughly a factor of three larger than the input previously used for  $\sigma_{\omega N}$  in models. A similar result had been previously reported from the LEPS collaboration for the  $\Phi$  meson [17]. In this case an absorption cross section of  $\approx 30$  mb was deduced, which has to be compared to the free nucleon absorption cross section of 7.7 - 8.7 mb. Both experiments give strong evidence for the much discussed in-medium modification of vector mesons.

An overview of the results for some mesons is summarized in Fig. 2. The absorption properties

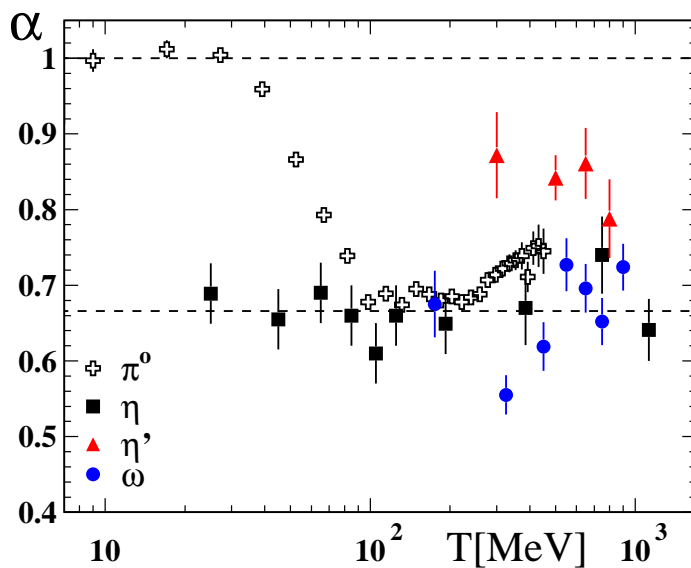


**Figure 2.** Scaling coefficients  $\alpha$  as function of kinetic meson energy  $T$  for  $\pi^0$ ,  $\eta$ ,  $\eta'$ , and  $\omega$  mesons.

vary for the different meson types. We shortly comment on some features which are relevant for experiments discussed later in this contribution. The absorption coefficient for pions has a pronounced energy dependence. The reason is, that as soon as pions reach a kinetic energy of  $\approx 100$  MeV they can excite a nucleon into the  $\Delta$ -resonance and are readily absorbed. Therefore, nuclei are basically ‘black’ for pions in this energy range. However, at low kinetic energies pions - the Goldstone bosons of chiral symmetry - interact only weakly with nucleons so that below kinetic energies of  $\approx 40$  MeV nuclei become transparent for pions. This behavior is important for the study of the in-medium invariant-mass distributions of pion pairs discussed below in view of in-medium modifications of the  $\sigma$  meson. Only pion pairs where both mesons have very small momenta are not significantly influenced by FSI effects. Another topic discussed below is the formation of mesic nuclei (quasi-bound systems of a nucleus and a meson). Due to the very weak low-energy interaction pions are obviously no candidates for such systems, but the situation is different for the heavier mesons, in particular the  $\eta$ -meson.

The low-momentum  $\eta$ -nucleon interaction is completely dominated by the  $s$ -wave excitation of the  $S_{11}(1535)$  resonance, which overlaps with the  $N\eta$  production threshold and has a  $\approx 50$  % decay branching ratio into  $N\eta$  [18]. Therefore, nuclei are ‘black’ for  $\eta$ -mesons even for almost vanishing momenta of the meson. As a side remark, this strong coupling to the  $S_{11}$  resonance with almost equal branching ratios to  $N\pi$  and  $N\eta$  provides also a very efficient mechanism for the production of secondary  $\eta$ -mesons in nuclei via the  $\gamma N \rightarrow N\pi$ ,  $\pi N \rightarrow N\eta$  reaction chain at somewhat higher incident photon energies [11, 12], which must be properly accounted for in the extraction of the  $\eta$ -absorption probabilities.

The special features of the  $N\eta$  interaction have already 25 years ago lead to speculations about the existence of so-called  $\eta$ -mesic nuclei. Liu and Haider [19], based on the results from coupled channel analyses of  $\eta$ -production reactions, suggested the possible formation of quasi-bound  $\eta$  - nucleus states for  $A > 10$  nuclei. Experimental evidence has been sought in pion induced reactions [20, 21], but those experiments did not produce conclusive evidence. More recently, Sokol and co-workers [22, 23] claimed evidence for the formation of  $\eta$ -mesic nuclei from bremsstrahlung induced reactions on  $^{12}\text{C}$

$$\gamma + ^{12}\text{C} \rightarrow p(n) + ^{11}_{\eta}\text{B}(^{11}\text{C}) \rightarrow \pi^+ + n + X \quad (2)$$

where the  $n\pi^+$  pairs were detected in the final state. The  $\eta$ -meson is produced in quasi-free kinematics on a nucleon (p,n) so that it is almost at rest in the residual  $A = 11$  nucleus. When a quasi-bound state was produced, the  $\eta$ -meson can be re-captured by a nucleon into the  $S_{11}$  excitation, which may then decay into a pion-nucleon back-to-back pair. Sokol and Pavlyuchenko [23] claim an enhancement above background from quasi-free pion production for certain kinematic conditions.

Suggestions for the existence of very light  $\eta$ -mesic states, in particular involving helium or tritium nuclei, were later based on results from refined analyses of the  $\eta$ -nucleon,  $\eta$ -nucleus scattering length (see [24] for a summary), using precise data from threshold  $\eta$ -photoproduction off the proton [25], the deuteron [26, 27, 28, 29], and helium nuclei [30, 31]. Such states have been in particular sought in the threshold behavior of hadron and photon induced  $\eta$ -production reactions from light nuclei, following the conjecture that a resonant state close to production threshold will enhance the cross section with respect to phase-space expectations. Particularly large effects have been observed for the  $dp \rightarrow \eta^3\text{He}$  [32, 33] reaction and for the  $\gamma^3\text{He} \rightarrow \eta^3\text{He}$  reactions. For the latter recently much more precise data have been measured at MAMI, which we will discuss below.

As a final remark to meson-nucleus interactions, we like to emphasize (see Fig. 2) that FSI effects seem to be considerably smaller for  $\eta'$  mesons than for the  $\eta$  and  $\omega$ . This might be a first indication that the  $\eta'$ -nucleon interaction is not strong, which is important in view of the discussion about the possible existence of mesic states for this heavy meson.

Finally, we will discuss very recent results related to the in-medium properties of the  $\sigma$ -meson. A possible in-medium mass shift of the  $\sigma$ -meson has been much discussed in connection with partial chiral symmetry restoration. The  $J^\pi = 0^+$   $\sigma$ -meson is the chiral partner of the  $J^\pi = 0^-$  pion, but in vacuum their masses are very different, which is a well-known manifestation of chiral symmetry breaking. The naive assumption that the two masses should become degenerate in the chiral limit is supported by model calculations. A typical result is the density dependence of the mass calculated in the Nambu-Jona-Lasino model by Bernard, Meissner and Zahed [35], who predicted a considerable lowering of the  $\sigma$ -mass already at normal nuclear matter density  $\rho_0$ , where the pion mass is still stable. Due to the strong coupling of the  $\sigma$  to scalar, isoscalar pion pairs an in-medium shift of its mass should be reflected in the invariant mass distributions of  $\pi^0\pi^0$  (and  $\pi^+\pi^-$ ) pairs [36, 37, 38, 39]. Such effects have been sought in pion induced reactions at the CHAOS spectrometer (see e.g. [40, 41]) and with the Crystal Ball detector at BNL [42], as well as with photon induced reactions at MAMI [43, 44]. All experiments found some in-medium effects. However, they might also arise from final state interactions of the pions. Originally, the different behavior of possible decay channels of the  $\sigma$  ( $\pi^0\pi^0$ ,  $\pi^+\pi^-$ ) on one hand side, and isospin-channels that cannot couple to the  $\sigma$  (e.g.  $\pi^+\pi^+$ ,  $\pi^0\pi^\pm$ ) on the other hand, was taken as strong argument that FSI effects alone cannot explain the data. However, later [44] it was shown that intricate side-feeding effects from charge-exchange scattering of the pions can mimic  $\sigma$  in-medium modifications. It is therefore highly desirable to study such effects for pions with very low kinetic energies (that is double pion production in the vicinity of the production thresholds) in order to avoid the FSI effects.

## 2. Experiments

The experiments have been done at the tagged photon facilities of the Bonn ELSA accelerator and the Mainz MAMI accelerator. At both facilities almost  $4\pi$  covering electromagnetic calorimeters combined with charged particle detectors have been used. The results discussed here have been obtained with unpolarized photon beams and unpolarized liquid or solid targets, but programs using linearly and circularly polarized beams and longitudinally and transversely polarized targets are also under way. A more comprehensive overview of experimental facilities for tagged photon experiments is given in [45].

### 2.1. The Crystal Barrel/TAPS setup at the Bonn ELSA accelerator

The electron stretcher accelerator facility ELSA [46, 47] delivers electron beams with energies up to 3.5 GeV and intensities of typically a few nA. Most of the experiments discussed here, have been done with the setup summarized in Fig. 3. The setup and the analysis procedures are discussed in detail in [48, 49]. The main detector was a  $4\pi$  electromagnetic calorimeter combining the Crystal Barrel [50] (1290 CsI (Tl) crystals of 16 radiation lengths  $X_0$  all mounted in a target pointing geometry) with the TAPS detector [51, 52]. The barrel covered the full azimuthal angle for polar angles between  $30^\circ$  and  $168^\circ$ . The forward angular range was covered by TAPS mounted as a wall comprising 528 BaF<sub>2</sub> crystals of hexagonal shape with an inner diameter of 5.9 cm and a length of 25 cm corresponding to 12  $X_0$ . The front face of the BaF<sub>2</sub> wall was located 1.18 m from the center of the targets, which were mounted inside the barrel, and each module of the detector was equipped with an individual plastic scintillator for charged particle identification. The TAPS wall was read out with photomultipliers while the barrel crystals were equipped with photodiodes, which did not deliver timing information. Therefore only hits in TAPS could be used in the first level trigger, which somewhat limited the detection efficiency of the device. This is not a disadvantage for measurements off the free proton, where in addition the proton can generate triggers in the ‘Inner-detector’ [53], a three-layer scintillating fiber detector surrounding the target at polar angles between  $28^\circ$  and  $172^\circ$ . It limits, however, the type of reactions that can be studied off quasi-free neutrons. Only reactions with large photon multiplicity have reasonable trigger efficiencies. For future experiments the trigger capability of the detector will be upgraded by a new readout system based on Avalanche PhotoDiodes (APDs), which can deliver time information and trigger signals.

For most of the experiments discussed here, a liquid deuterium target was mounted inside the barrel. The more recent measurements with a polarized d-butanol target were done with a slightly modified setup, using a smaller TAPS wall combined with a forward plug of the barrel of CsI crystals equipped with photomultipliers [45].

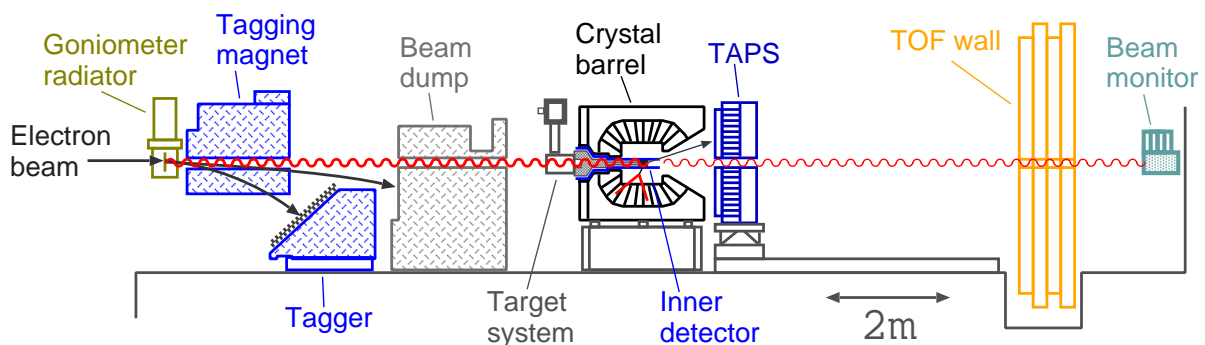


**Figure 3.** Experimental setup at the Bonn ELSA accelerator combining the Crystal Barrel detector, the TAPS detector as forward wall, inner detectors, and the photon tagging facility.

## 2.2. The Crystal Ball/TAPS setup at the Mainz MAMI accelerator

The MAMI accelerator in Mainz [54, 55] can now deliver electron beams with energies up to 1.5 GeV, however for some of the experiments lower beam energies have been used (883 MeV). Like at ELSA photon beams are produced by the bremsstrahlung process and are tagged with the Glasgow magnetic spectrometer [56]; at maximum electron energy with a typical resolution of 4 MeV (2 MeV for 883 MeV electron beam energy). Since the accelerator is designed also for electron scattering experiments, it can deliver electron beam intensities far larger than needed for tagged photon experiments ( $\approx 100 \mu\text{A}$ , compared to some tens of nA used for tagging). For the experiments discussed here, Liquid hydrogen, liquid deuterium, liquid  $^3\text{He}$ , and solid lithium, carbon, calcium, and lead targets have been used.

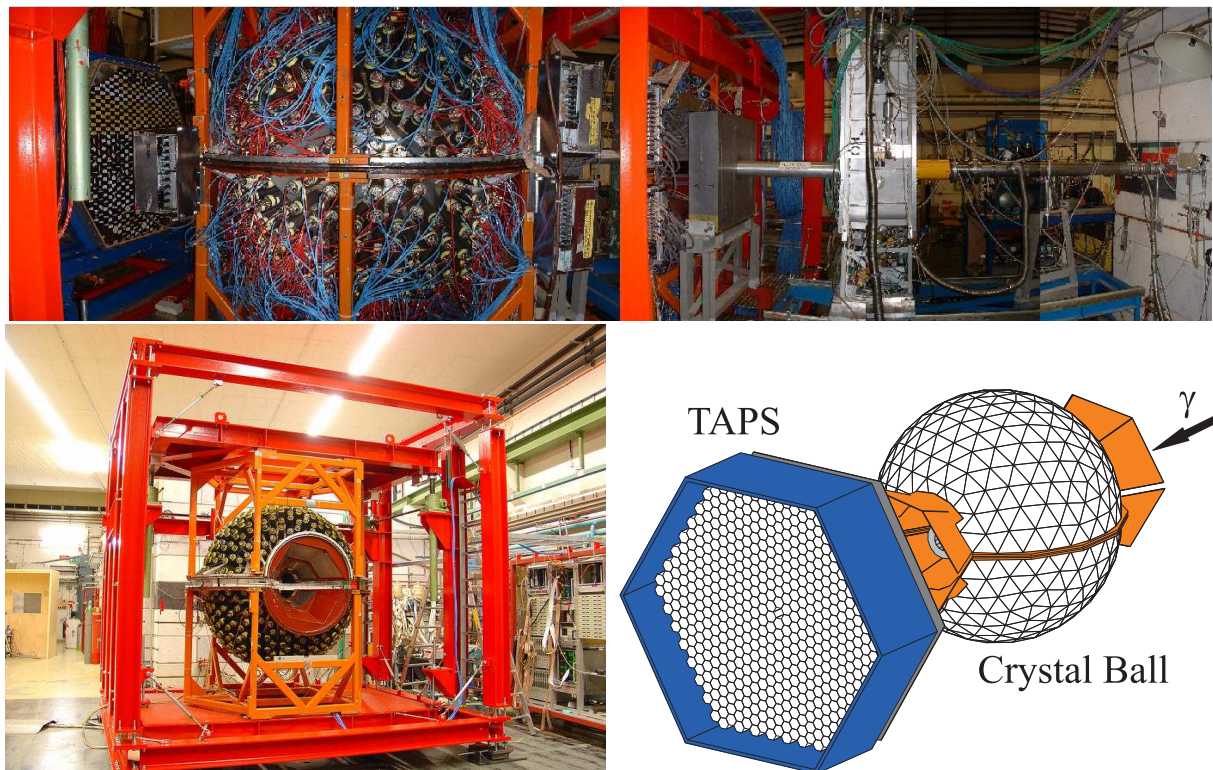


**Figure 4.** Overview of the MAMI setup. Upper part: beam coming from the right, Crystal Ball at the left of the picture, TAPS forward wall at the very left. Bottom part, left hand side: Crystal Ball in setup phase, right hand side: schematic drawing of the calorimeter.

The electromagnetic calorimeter (see Fig. 4) combined the Crystal Ball detector [57] and part of the TAPS detector. The Crystal Ball detector consists of 672 NaI crystals covering the full azimuthal angle for polar angles from  $20^\circ$  to  $160^\circ$ . For the TAPS forward wall, which covered angles from  $21^\circ$  to  $2^\circ$ , two different configurations have been used. The first was built from 510  $\text{BaF}_2$  crystals and placed at a distance of 1.75 m from the target center, the second comprised 384 elements and was placed at 1.457 m from the target. Both versions provided good resolution for time-of-flight and ToF-versus-energy measurements for particles detected in TAPS. The TAPS modules were again equipped with individual plastic scintillators for charged particle detection. The target inside the Ball was surrounded by a particle detection detector (PID) [58], which via  $E - \Delta E$  measurements, comparing the energy loss in the PID and the deposited energy in the Ball, allowed also for separation of protons and charged pions. A detailed discussion of the setup and analysis procedures is given in [59].

### 3. Results and Perspectives

In this section we will summarize recent results, some of which are already published, but most are in preparation for publication and shortly indicate the direction of planned or already running follow-up experiments.

#### 3.1. Quasi-free photoproduction of mesons off the neutron

Before we present the results for some selected recently studied meson production channels, we will shortly discuss some general issues, arising for the measurement of meson production reactions of quasi-free nucleons. The most important issues are:

- How well are the systematic uncertainties involved in the detection of mesons in coincidence with recoil neutrons and protons understood?
- How can we best deal with the effects of nuclear Fermi motion?
- What is the importance of other effects related to the nuclear environment like e.g. FSI?

These questions have been studied in detail for the measurements done at the Bonn facility (the data from MAMI are all still under analysis), using data from  $\eta^-$  [49],  $\eta'^-$  [48],  $2\pi^0-$ , and  $\pi^0\eta$  production. We discuss here as an example the  $\eta$ -channel.

The electromagnetic calorimeters at both facilities are well capable of also detecting recoil protons and neutrons, although with very different detection efficiencies (up to 90 % for protons roughly 15 - 30 % for neutrons). Separation of photons, protons, and neutrons in the TAPS forward walls can be achieved with the help of the thin plastic scintillators in front of the BaF<sub>2</sub> modules, pulse-shape analysis, and time-of-flight, respectively ToF-versus-energy methods. Separation of protons from photons and neutrons can be done with the charged particle detectors surrounding the target, but no separation between photons and neutrons detected in the Barrel or Ball is possible (time-of-flight path too short). Therefore, the only possible strategy to analyze reactions in coincidence with such recoil neutrons is to accept events with (n+1)-neutral hits, where n is the number of expected photons. Then test the reaction hypothesis by looking at all possible invariant mass combinations of those hits (for example for  $\eta \rightarrow 3\pi^0 \rightarrow 6\gamma$  three photon pairs must combine to invariant masses close to the  $\pi^0$ -mass and the invariant mass of these six photons should be close to the  $\eta$ -mass). In case of more than one possible combination the 'best' one is selected by a  $\chi^2$  test, and in the end the left-over neutral hit is tentatively accepted as recoil neutron. This procedure must be precisely reproduced by simulations for the reaction detection probability, which is not straight forward since already the simulation of the detector hardware response to neutrons is notoriously difficult. In case of recoil protons, detection efficiencies can be easily extracted using production reactions off free protons, but there are not many possible reactions one can use in the case of neutrons ( $\gamma p \rightarrow n\pi^0\pi^+$  is one of the best suited). As far as the detector response to neutrons is concerned, simulations with the GCALOR program package [60] provide rather satisfactory results, but also they require very careful control of all parameters (in particular detector thresholds).

Therefore it is extremely helpful, that an intrinsic control exists. The cross sections for meson production off the deuteron (or other light nuclei) must obey the relation:

$$\sigma_{incl} = \sigma_p + \sigma_n + \sigma_{coh} \quad , \quad (3)$$

where  $\sigma_{incl}$  is the inclusive cross section without any condition for recoil baryons,  $\sigma_p$ ,  $\sigma_n$  are the cross sections in coincidence with recoil protons and neutrons, and  $\sigma_{coh}$  is the coherent production cross section off the respective nucleus. In most cases, the latter one is completely negligible in comparison to the quasi-free reactions, which we will assume in the following discussion (if it is not, it can be also measured). This means, that the two exclusive cross sections with coincident protons and neutrons have to add up to the inclusive cross section. Only

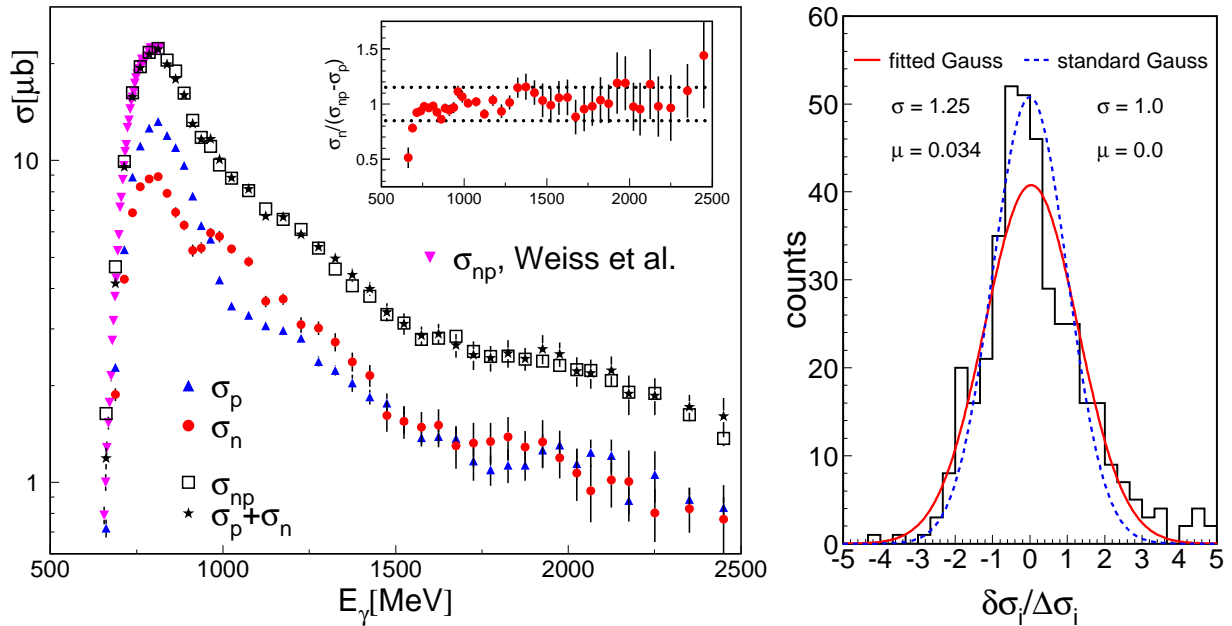


**Figure 5.** Comparison of cross sections for quasi-free  $\eta$  photoproduction [49]. Left hand side: total cross sections, (Blue) upward triangles: quasi-free proton cross section  $\sigma_p$ , (red) dots: quasi-free neutron cross section  $\sigma_n$ , (black) open squares: inclusive quasi-free cross section  $\sigma_{np}$ , (black) stars:  $\sigma_n + \sigma_p$ . Downward (magenta) triangles: inclusive quasi-free cross section from Weiss et al. [29]. Inset: ratio of neutron cross sections. Right hand side: Distribution of deviations between  $d\sigma_n/d\Omega$  and  $d\sigma'_n/d\Omega = d\sigma_{incl}/d\Omega - d\sigma_p/d\Omega$ . Solid (red) curve: fitted Gaussian distribution (width  $\sigma=1.25$ , mean  $\mu=0.034$ ), dashed (blue) curve: standard Gauss: ( $\sigma=1$ ,  $\mu=0$ ).

the detection efficiency for the mesons enter into the inclusive cross section. The completely different proton and neutron detection efficiencies enter into  $\sigma_p$  and  $\sigma_n$  so that Eq. 3 in general holds only when all detection efficiencies are correct. This means that the neutron cross section can be measured in two different ways, either as  $\sigma_n$  by the detection of recoil neutrons or as difference  $\sigma'_n = \sigma_{incl} - \sigma_p$ . The result of such an analysis for  $\eta$ -production from the Crystal Barrel/TAPS experiment [49] is shown in Fig. 5. The left hand side of the figure demonstrates the agreement of the total cross sections. The right hand side of the figure shows the distribution of the deviations  $\delta\sigma_i$  normalized by the statistical uncertainties  $\Delta\sigma_i$

$$\frac{\delta\sigma_i}{\Delta\sigma_i} \equiv \frac{d\sigma'_n/d\Omega - d\sigma_n/d\Omega}{\sqrt{\Delta^2(d\sigma'_n/d\Omega) + \Delta^2(d\sigma_n/d\Omega)}} \quad (4)$$

for all data points (420 entries) of the angular distributions from production threshold to 2.5 GeV, compared to a Gaussian distribution, which is fairly close to a standard Gaussian distribution. Very similar results have been obtained for  $\eta'$  production [48] and  $\pi^0\pi^0$  production (in preparation). In case of reactions with very small cross sections, it may be useful to use  $\sigma'_n$  instead of  $\sigma_n$ , because of better statistical quality. In the extreme, one may even attempt to measure  $\sigma''_n$ , where only events *without* recoil protons are accepted, provided proton acceptance and detection efficiency can be pushed above the  $\approx 90\%$  level and the corresponding background contribution to  $\sigma''_n$  can be simulated. Since neutron detection efficiencies are typically below the 30% limit, this would increase count rates by approximately a factor of three. The disadvantage of this indirect methods is, that the kinematic reconstruction discussed below for the elimination of Fermi motion effects is then not possible.

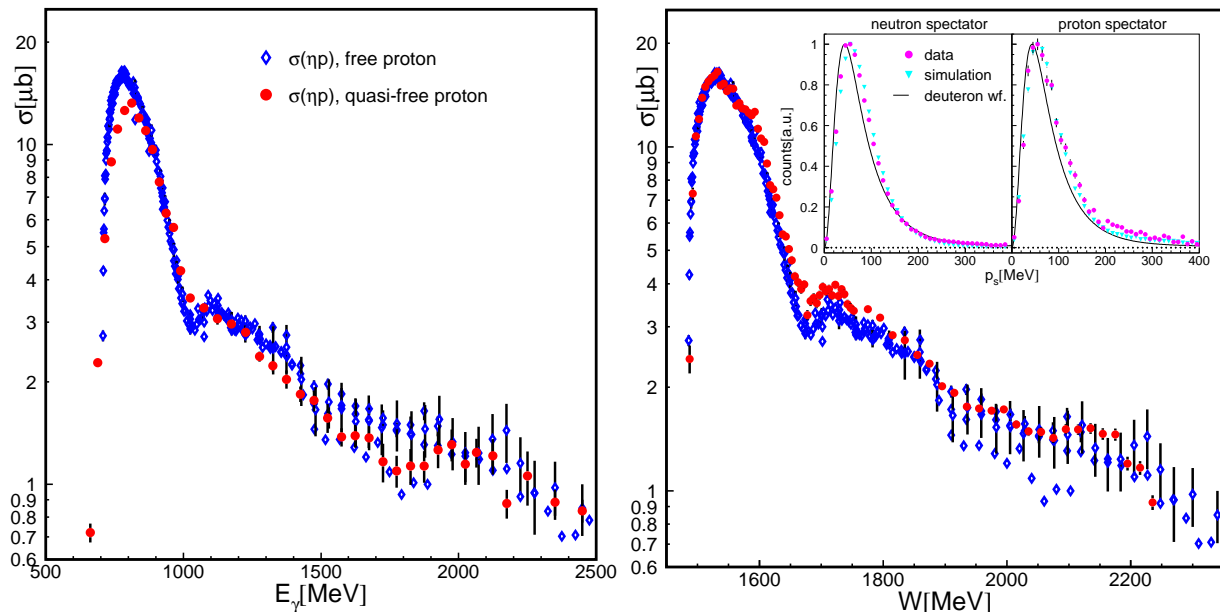


**Figure 6.** Comparison of free and quasi-free photoproduction of  $\eta$ -mesons off the proton (see text). Left hand side: (Blue) diamonds world data base for  $\gamma p \rightarrow p\eta$  versus incident photon energy. (Red) dots: quasi-free  $\gamma'p' \rightarrow p'\eta$  reaction. Right hand side: Free proton data (blue diamonds) versus  $W$ . (Red) dots: quasi-free data from kinematic reconstruction of  $W$ . Insert: reconstructed momenta of spectator nucleons compared to momentum distributions from deuteron wave function (neutron spectator corresponds to detection of recoil proton and vice versa). Curve: deuteron wave function, simulation includes detector resolution.

The influence of Fermi motion is shown for the reaction  $\gamma p \rightarrow p\eta$  in Fig. 6, where at the left hand side the total cross sections for free protons and protons bound in the deuteron are compared as function of incident photon energy. The results are similar, but the slope at threshold is less steep, the maximum of the  $S_{11}$  peak is underestimated, and the little dip-like structure around 1 GeV is smeared away in the quasi-free data; all typical effects of Fermi motion. These effects can be removed when instead of the incident photon energy (or  $W$  calculated from it neglecting Fermi motion), the invariant mass  $W$  calculated from the measured four-vectors of the recoil nucleon and the meson is used. In this case, in principle angle and kinetic energy of the recoil nucleon are needed, which is straight forward for the proton, but less so for the neutron. At forward angles it can be measured by time-of-flight methods, but not for neutrons in the Barrel or Ball. However, since the incident photon energy is known and the incident deuteron is at rest, the three-body final state (meson, participant, and spectator nucleon) is already kinematically completely determined by the mass of all three particles, the three-momentum vector of the meson, and the angles of the participant nucleon. The four missing variables (three-momentum of the spectator, kinetic energy of the participant nucleon) can be calculated from energy and momentum conservation. An example is shown at the right hand side of Fig. 6. The insert in the figure shows the momenta of the spectator nucleons derived from the kinematic reconstruction. As long as FSI effects are negligible and the reaction kinematics was quasi-free, they should correspond to the momentum distribution of the nucleons bound in the deuteron, which can be derived from the deuteron wave function [61]. As shown in the figure, the agreement is excellent when the instrumental resolution is taken into account. The main plot then demonstrates the very good agreement between free and quasi-free data, which also implies that effects beyond Fermi smearing (FSI) play no significant role for the  $\eta$ -channel.

In the following we will discuss results from a few selected channels in view of their physical interpretation.

*3.1.1. photoproduction of  $\eta$ -mesons* Photoproduction off  $\eta$ -mesons off the free proton has been studied during the last two decades in much detail by all laboratories running tagged photon experiments [25, 62, 63, 64, 65, 66, 67, 68, 69, 70, 71, 72, 73, 74, 75, 76, 77]. The main results were the strong dominance of the  $S_{11}(1535)$  in the threshold region, with only small contributions from non-resonant background terms, a destructive interference between the  $S_{11}(1535)$  and the  $S_{11}(1650)$  at somewhat higher incident photon energies, and a small contribution from the  $D_{13}(1535)$  resonance. The latter showed up in a detailed analysis of the angular distributions [25, 29] via an interference with the leading  $S_{11}$  excitation; but the effect was more pronounced for the beam asymmetry measured with linearly polarized photons [62, 72] and an analysis in the framework of the ‘Eta-MAID’ model [78] allowed the extraction of the tiny  $N\eta$  branching ratio ( $0.23 \pm 0.04$  %) [2] of the  $D_{13}$  resonance. The situation is less clear above this range, where different analyses like Eta-MAID [78] and Bonn-Gatchina (BoGa) [79] propose different resonance contributions (see e.g. [72]).

Measurements of the  $\gamma n \rightarrow \eta n$  reaction were originally mainly motivated as an almost background free study of the isospin composition of the electromagnetic excitation of the  $S_{11}(1535)$  resonance. Furthermore, for the energy range above the  $S_{11}$ , there were predictions [78] for a strong contribution from the  $D_{15}(1675)$  resonance, which is suppressed for the proton due to the Moorehouse selection rules [81] for electromagnetic excitations. Early results [26, 27, 28, 29], covering only the  $S_{11}$  range (mainly up to 900 MeV), basically confirmed expectations and yielded a precise value for the ratio of proton and neutron electromagnetic couplings of the  $S_{11}(1535)$  [80]. But there was a large surprise when the experiments reached incident photon energies above 1 GeV: all cross section measurements extending into this region [82, 83, 84] found a significant and relatively narrow structure in the excitation function. The result from the ELSA experiment [84, 49] is summarized in Figs. 7,8. The structure is located around an invariant mass of  $W \approx 1.65$  GeV with a width below 50 MeV. At the time when it was first seen in experiment, the possible discovery of exotic pentaquark states was hotly debated and models predicted that the  $P_{11}$ -like state of the anti-decuplet should couple electromagnetically much more strongly to the neutron than to the proton, have a large branching ratio into  $N\eta$ , and mass/width comparable to the observations of the structure in  $\eta$ -photoproduction. However, in the meantime evidence for the

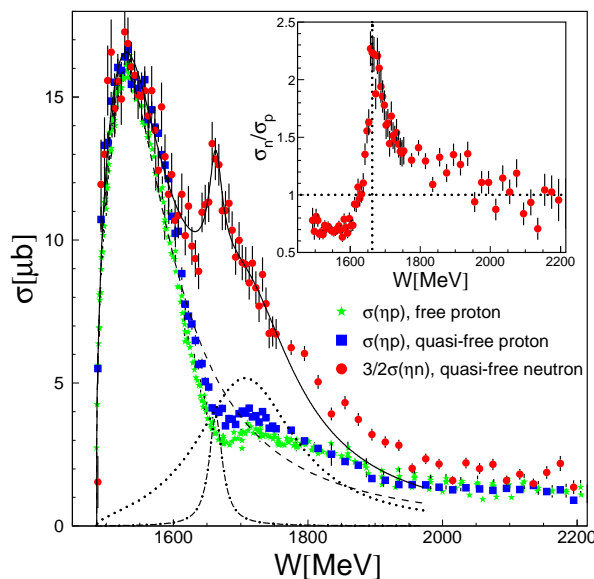


**Figure 7.** Quasi-free photoproduction of  $\eta$ -mesons off the proton and neutron [49]. Main plot: Total cross sections as function of the final state invariant mass  $W$  reconstructed from measured four-vectors (Red) dots: quasi-free neutron, (blue) squares: quasi-free proton, (green) stars: free proton data. The quasi-free neutron data are normalized to the proton data in the  $S_{11}$  peak (factor  $\approx 2/3$ ). All curves for neutron data; dashed: fitted  $S_{11}$  line shape, dotted: broad Breit-Wigner resonance, dash-dotted: narrow Breit-Wigner, solid: sum of all. Inset: ratio of quasi-free neutron - proton data.

$\Theta^+$  pentaquark has faded and many attempts for alternative explanations of the results from  $\gamma n \rightarrow \eta n$  have been made [85, 86, 87, 88, 89], ranging from intricate interference effects over threshold cusps to nucleon resonances with different properties. The data reconstructed from the final state kinematics and thus not effected by nuclear Fermi motion have only ruled out an explanation involving only a normally broad (i.e. typically  $>150$  MeV) nucleon resonance. Apart from that the nature of this structure is still unknown.

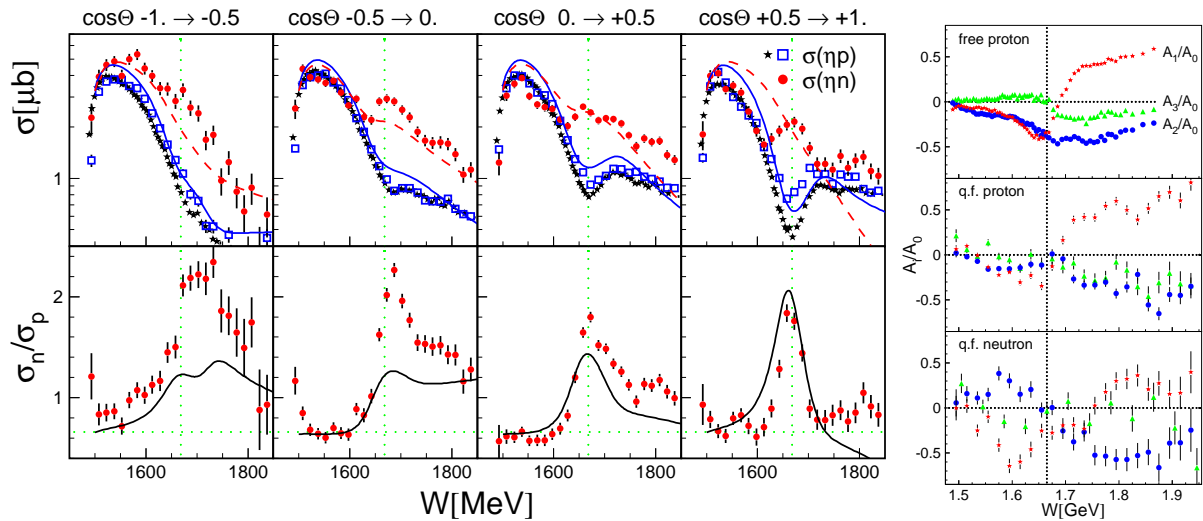


**Figure 8.** Quasi-free photoproduction of  $\eta$ -mesons off the proton and neutron [49]. Left hand side: First row: excitation functions for different bins of  $\eta$  cm polar angle. (Blue) open squares: quasi-free proton data, (black) stars: free proton data from [77], (red) dots: quasi-free neutron data scaled up by  $3/2$ . (Blue) solid lines:  $\eta$ -MAID [78] for the proton target, (red) dashed lines:  $\eta$ -MAID for the neutron target. Second row: ratio of neutron and proton cross section for data and  $\eta$ -MAID. Vertical dotted lines: position of narrow peak in neutron data, horizontal dotted lines:  $\sigma_n/\sigma_p=2/3$ . Right hand side: coefficients of Legendre series fitted to angular distributions normalized to  $A_0$ . From top to bottom: free proton [77], quasi-free proton, quasi-free neutron [49].

Some additional information comes from the angular dependence shown in Fig. 8 [49]. The excitation functions for different ranges of  $\eta$  cm angle show a clear angular dependence of the effect. It is most prominent for forward angles. Moreover, the peak-like structure in the neutron data corresponds to a dip-like structure in the proton data with similar angular dependence. This might be an indication that at least at some level an interference term with opposite sign for proton and neutron contributes. It is noteworthy, that the MAID model [78], which reproduces at least for forward angles qualitatively the neutron/proton cross section ratio, does so only because it reproduces the ‘dip’ in the proton data (because it has been fitted to it) but not the peak in the neutron data. This causes also some doubts, whether the parameterization of the proton data reflects the correct physics. The coefficients of the Legendre polynomials fitted to the data and normalized to the leading coefficient  $A_0$ , which is proportional to the total cross section, show that for both, proton and neutron there is a dramatic change in the angular dependence around the position of the discussed structures. So far, there are no models available which reproduce this behavior.

The significance of the structure has been further increased with new data from the MAMI facility for  $\eta$ -photoproduction off quasi-free nucleons from the deuteron but also from  $^3\text{He}$ . The data are still under analysis and the much superior statistical quality of the deuteron data will

allow more precise investigations of the angular dependencies. Preliminary excitation functions are shown in Fig. 9. The data taken with the helium target are a further stringent test that no systematic problems influence the data. They behave exactly as expected, although extracted from a much more challenging environment (larger Fermi motion, proton/neutron ratio 2:1). The somewhat worse resolution for helium in the data with reconstructed final state kinematics is due to the fact that the reconstruction is only exact for the three-particle final state from the deuteron target, but has to rely on the approximation of zero relative momentum between the two spectator nucleons in the helium case.

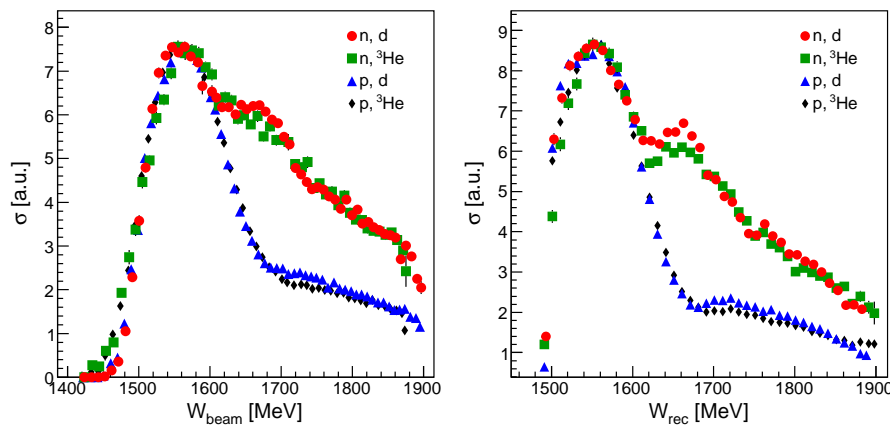


**Figure 9.** Preliminary excitation functions for quasi-free protons and neutrons from  $^2\text{H}$  (only small fraction of total statistics) and  $^3\text{He}$ . Left hand side:  $W$  from incident photon energy, right hand side:  $W$  from final state invariant mass.

More detailed partial wave analysis of the data will require the measurement of polarization observables. So far, only the beam asymmetry  $\Sigma$  has been measured for  $\gamma n \rightarrow \eta n$  by the GRAAL collaboration [90]. More recently, first data have been taken at ELSA to measure the helicity dependence of the cross section with a longitudinally polarized d-buthanol target and a circularly polarized photon beam. At MAMI first data have been taken with a transversely polarized d-buthanol target and a circularly polarized beam to measure the target asymmetry  $T$  and the double polarization observable  $F$ . These data are still in a very early state of analysis and measurements will continue to collect more counting statistics.

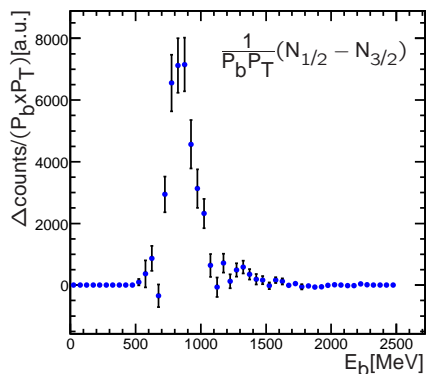


**Figure 10.** Very preliminary (almost online) result for the count rate difference (normalized to polarization degrees) for  $\sigma_{1/2}$  (anti-parallel photon-proton spin) and  $\sigma_{3/2}$  (parallel spins) for  $\eta$  photoproduction off quasi-free protons from the deuteron.

Figure 10 shows an example for the measurement of the helicity dependence of the cross section (online data) for quasi-free protons as demonstration of the feasibility of these experiments. Apart from a little effect of Fermi smearing the result is in good agreement with free proton data [91]. It shows the expected dominance of the  $\sigma_{1/2}$  component in the  $S_{11}$  range. Analysis of the neutron data is expected to reveal whether the structure is related to  $J = 1/2$  or to  $J > 1/2$  partial waves.

*3.1.2. photoproduction of  $\eta'$ -mesons* Another channel that has recently attracted much interest in view of nucleon resonances is the  $N\eta'$  final state. Like the  $\eta$ , also the isoscalar  $\eta'$  couples only to isospin-1/2  $N^*$  resonances. Due to its large mass the free-nucleon threshold is at  $E_\gamma \approx 1447$  MeV, corresponding to  $W \approx 1.9$  GeV. This means that it is well suited to search for contributions from  $N^*$  resonances around  $W=2$  GeV, i.e. in the nucleon excitation range with a large density of ‘missing’  $N^*$  resonances. Since this region is still close to the production threshold one might expect that only few partial waves contribute, which would simplify the interpretation of the data. For the free proton, apart from old bubble chamber data, first results became available from the SAPHIR experiment at ELSA [92]. Subsequently, much more precise data have been reported from the CLAS experiment at Jlab [93, 74] and the Crystal Barrel/TAPS setup at ELSA [75]. Interpretation of these data is still controversial [94, 95]; almost all model fits agree that close to threshold there is an important contribution from an  $S_{11}$  resonance and at higher energies  $t$ -channel background processes are significant but other resonance contributions are not well constrained by the measured angular distributions alone. Future measurements of polarization observables are mandatory.

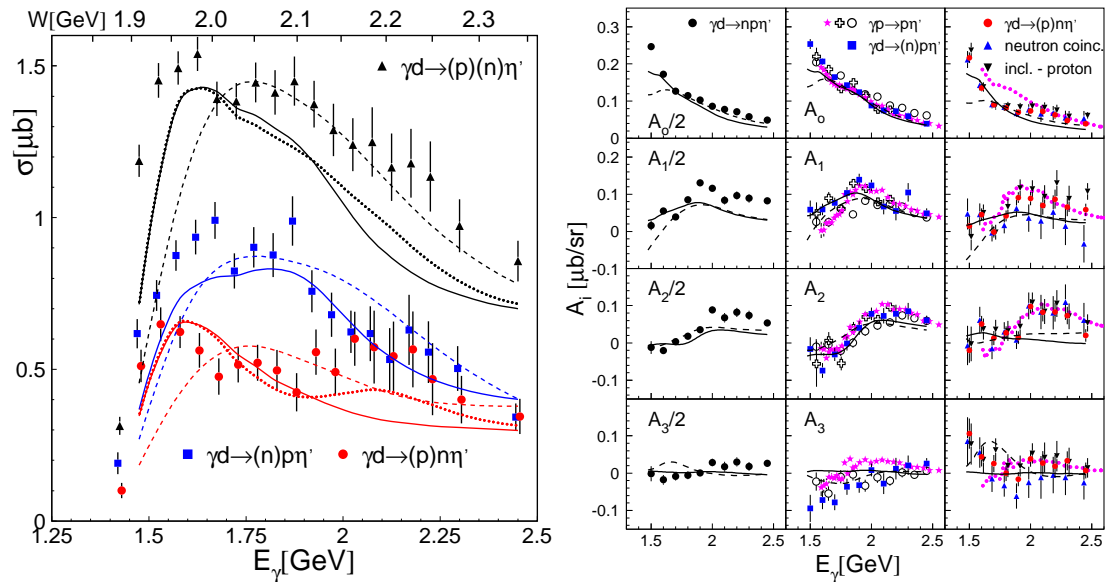


**Figure 11.** Left hand side: Total cross section for  $\eta'$  production off the deuteron. [48]. Curves: fits with reaction models, solid, dotted: different solutions from [95], dashed:  $\eta'$ -MAID [94]. Right hand side: Coefficients of the Legendre Polynomials for the fitted angular distributions [48]. Left hand column: inclusive reaction scaled down by factor of 2. Center column (proton targets): quasi-free data (blue squares); free proton data: open crosses [93], open circles [75], (magenta) stars [74]. Right hand column (quasi-free neutron data): (blue) upward triangles from neutron coincidence, (black) downward triangles from difference of inclusive and proton data, (red) circles from averaged data. In all plots solid lines: NH model, dashed lines:  $\eta'$ -MAID; for neutron: (magenta) dotted lines CLAS proton data.

The first measurement of the  $\gamma n \rightarrow \eta' n$  reaction was recently published [48] from the CBELSA/TAPS experiments, using a liquid deuterium target. Total cross sections and Legendre coefficients of the angular distributions are summarized in Fig. 11. Also in this case good agreement between free and quasi-free proton data was found (i.e. no significant FSI) and the behavior of proton and neutron cross sections points to different resonance contributions. However, also for the neutron target, model solutions are not unique and constraints from polarization observables are needed.

*3.1.3. photoproduction of  $\pi^0$ -mesons* Photoproduction of pions in the  $\Delta$ -resonance region and throughout the second and third resonance regions of the nucleon is one of the best studied meson production channels; however also in this case the data base for the all-neutral final state  $n\pi^0$  is very sparse [45]. So far, isospin decompositions rely on measurements of the  $\gamma n \rightarrow p\pi^-$  reaction, but since the non-resonant backgrounds can be very different for charged and neutral mesons, this is unsatisfactory. However, it is known that at least in the range of the  $\Delta$ -resonance FSI effects for  $\pi^0$  production off the deuteron are significant [98, 99]. This is not unexpected, already the relatively large contribution from coherent reaction processes in this energy range [98] highlights the importance of nuclear effects. The situation at higher incident photon energies is much less well understood, so far neither exclusive data nor model results including FSI effects were available. The only hint came from a measurement of inclusive  $\pi^0$  production off the deuteron in the second resonance region [98]. These data were significantly overestimated by simple plane wave approximations using as input the results of the MAID [96] or SAID [97] analyses for the elementary cross sections.

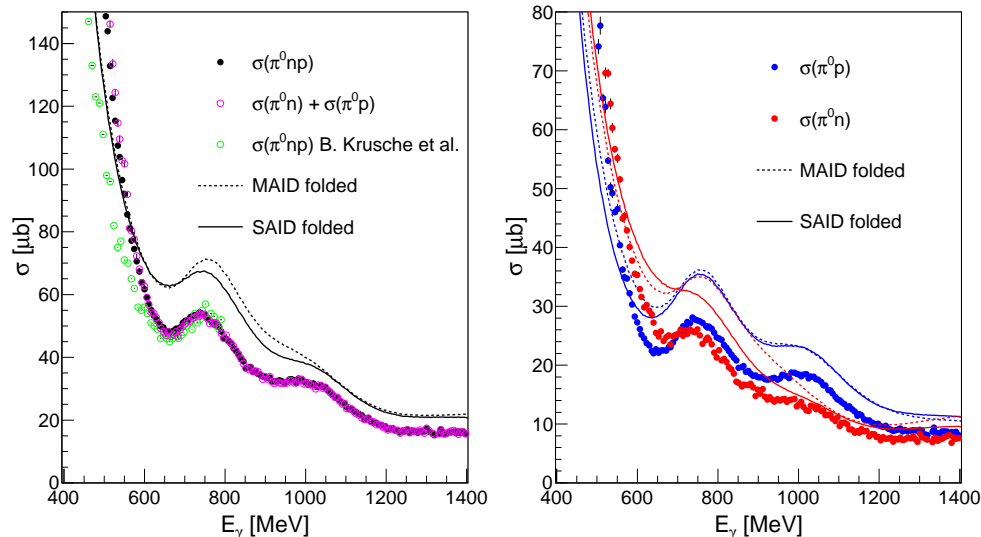


**Figure 12.** Very preliminary results for quasi-free photoproduction of  $\pi^0$  mesons off the deuteron in the second and third resonance region. Left hand side: inclusive  $\gamma d \rightarrow np\pi^0$  data compared to the sum of exclusive cross sections and results from MAID (dashed line) [96] and SAID (solid line) [97]. Both model results are for the incoherent sum of proton/neutron cross sections folded with Fermi motion. Right hand side: Same for exclusive quasi-free  $\gamma p \rightarrow p\pi^0$  and  $\gamma n \rightarrow n\pi^0$  reactions.

New exclusive data from the Crystal Ball/TAPS experiment, which are still under analysis, seem to confirm this observation. Preliminary results are summarized in Fig. 12. The left hand side shows the inclusive cross section  $\gamma d \rightarrow np\pi^0$  constructed in two ways, either by an analysis without any conditions for recoil nucleons or as sum of the quasi-free neutron and proton cross sections measured in coincidence with recoil nucleons (coherent contributions are very small in this energy range). The two results agree and agree in the overlap region also reasonably well with the result from [98]. However, they do not agree with the incoherent sum of the MAID and SAID results for the elementary cross sections folded with Fermi motion. The right hand side of the figure shows the exclusive, quasi-free proton and neutron cross sections. In both cases, they do not agree with the MAID and SAID results. Since those are fitted to the free proton

data, this indicates a significant nuclear effect for the quasi-free proton data (and probably a similar effect for the neutron data). Nevertheless the comparison of proton and neutron data confirms the expected differences in resonance excitations, in particular in the third resonance region. These results are still preliminary, further cross checks of the absolute normalization of the data are still under way. The final results will provide precise angular distributions for both quasi-free reactions and thus allow detailed tests of FSI effects and give stringent inputs for the extraction of resonance couplings for the neutron.

*3.1.4. further channels under analysis* New data sets from ELSA and MAMI are also under analysis for quasi-free production of meson pairs, in particular the double pion channels ( $\pi^0\pi^0$ ,  $\pi^0\pi^\pm$ ) and the  $\pi\eta$ -channels ( $\pi^0\eta$ ,  $\pi^\pm\eta$ ). First, preliminary results seem to indicate that FSI effects are small for double pion production but substantial for the  $\pi\eta$ -channels. Since coherent contributions are small for the double pion channels but relatively large for the  $\pi\eta$  final states, this seems to be in line with the findings for single  $\eta$ ,  $\eta'$ , and  $\pi^0$  production.

### 3.2. $\eta$ -mesic nuclei

The search for  $\eta$ -mesic states with meson photoproduction can be done in two different ways. In quasi-free photoproduction of  $\eta$ -mesons kinematic conditions can be selected such that the momentum of the incident photon is carried away by the participant nucleon and the  $\eta$ -meson is produced (almost) at rest in the  $A - 1$  residual nucleus, or coherent  $\eta$ -production close to threshold off the  $A$  initial state nucleus can be used as entrance channels. In the latter case nuclei with quantum numbers that allow coherent  $\eta$ -production (i.e.  $I, J \neq 0$ ) must be used [80]. For light nuclei, the only promising candidates are  ${}^3\text{He}$ ,  ${}^3\text{H}$ , and  ${}^7\text{Li}$ , but the radioactive tritium is not considered for practical reasons. In a previous experiment Pfeiffer and collaborators [34] had found some evidence for the formation of  $\eta$ -mesic  ${}^3\text{He}$  in two different experimental signals.

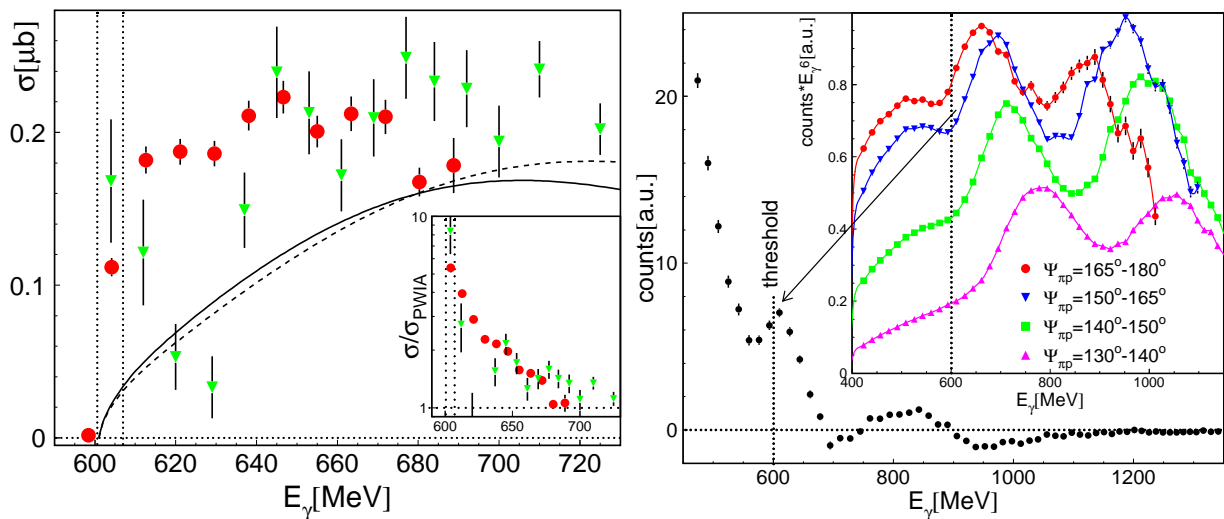


**Figure 13.** Left hand side: Total cross section for  $\gamma^3\text{He} \rightarrow \eta^3\text{He}$  (averaged over  $2\gamma$  and  $3\pi^0$  decays) (red dots) compared to previous data [34] (green triangles). Solid (dashed) curves: PWIA with realistic (isotropic) angular distribution for  $\gamma n \rightarrow n\eta$ . Inset: ratio of measured and PWIA cross sections. Right hand side: Main plot: difference of excitation functions of  $\pi^0 - p$  back-to-back pairs with opening angles between  $165^\circ - 180^\circ$  and  $150^\circ - 165^\circ$ . Inset excitation functions for different ranges of the opening angle  $\Psi_{\pi p}$  after removal of the overall energy dependence  $\propto E_\gamma^{-6}$ . Vertical dotted lines: coherent  $\eta$ -production threshold.

The total cross section of coherent  $\eta$ -production showed an extremely rapid rise at production threshold, far beyond phase-space expectation, and the angular distributions close to threshold were much more isotropic than expected from the influence of the nuclear form-factor. Furthermore, a tiny peak-like structure at  $\eta$ -production threshold in the excitation function of  $\pi^0 - p$  pairs emitted back-to-back in the photon-nucleus cm system was related to the reaction chain where a quasi-bound  $\eta$ -meson is re-captured by a nucleon into the  $S_{11}$  excitation with subsequent decay to  $N\pi$ . However, both signals suffered from very low counting statistics.

In a follow-up experiment [100] we have remeasured these reactions with Crystal Ball/TAPS at MAMI with much higher statistical precision. In addition, also the systematic uncertainties could be reduced due to two improvements. The almost  $4\pi$  coverage of the detector allowed a significant reduction of background from quasi-free  $\eta$ -production due to the detection of recoil nucleons. The large solid-angle coverage allowed in addition the measurement of not only the  $\eta \rightarrow 2\gamma$  decay but also the  $\eta \rightarrow 3\pi^0 \rightarrow 6\gamma$  decay branch could be used. The result for the total cross section is summarized in Fig. 13 and compared to the previous result and phase-space expectations. The overall agreement with the previous data is good, but there is a discrepancy around incident photon energies of 620 MeV. The old data showed a dip-like structure in this region which could not be reproduced. It is very probably due to systematic effects in the separation of the coherent reaction from breakup background in the previous experiment. The data confirm the extremely steep rise of the cross section at the coherent production threshold which is very unlike phase-space behavior. In addition also the behavior of the threshold angular distributions (not shown) disagrees strongly with plane-wave approximations.

The difficulty for the analysis of the  $\pi^0 - p$ -back-to-back pairs is background from quasi-free single-pion production. The approach for the previous experiment [34] was to subtract from the excitation function of back-to-back pairs (opening angles  $>170^\circ$ ) a normalized result for opening angles from  $150^\circ - 170^\circ$ , assumed to represent the background. A similar analysis of the present data (main plot at right hand side of Fig. 13) reproduces the previously observed peak with much higher statistical significance. However, closer inspection of the excitation functions for different ranges of opening angle (insert of the figure) shows that this peak-like structure is an artifact, arising from the structures related to quasi-free pion production in the second and third resonance region, which move upwards in photon energy for decreasing opening angles (a purely kinematic effect). Due to this, the difference of back-to-back pairs and pairs with somewhat smaller opening angles, just by chance has a peak-like structure at the  $\eta$ -threshold. Evidence for this second decay channel of an  $\eta$ -mesic resonance could thus not be confirmed.

Data of the same kind for  ${}^7\text{Li}$  nuclei have also been taken and are currently still under analysis.

### 3.3. Photoproduction of pion pairs from nuclei

The main motivation for this experiment [101] was to measure double pion production ( $\pi^0\pi^0$  and  $\pi^0\pi^\pm$  final states) from very light (deuteron and  ${}^7\text{Li}$ ) to heavy nuclei (Pb) with such high statistical quality that the invariant mass distributions of the pion pairs can be studied also close to production thresholds where, as discussed in the introduction, FSI effects are small. This can be directly verified again by an investigation of the scaling behavior of the total cross sections as function of the incident photon energy, which is shown in Fig. 14. Very close to threshold the cross sections scale in fact with the nuclear mass number  $A$ , indicating almost vanishing absorption effects and thus small FSI. The scaling coefficient  $\alpha$  then drops with increasing photon energy and approaches ‘surface-scaling’ ( $\alpha \approx 2/3$ ) around incident photon energies of 500 MeV. Invariant mass distributions of the pion pairs for both reactions and for different ranges of incident photon energy are summarized in Fig. 15. The shapes of the distributions are very similar for low incident photon energies and develop an enhancement of strength at small invariant masses for heavy nuclei only in the region where the FSI effects become large. Consequently, FSI seems to be a major source of these effects.

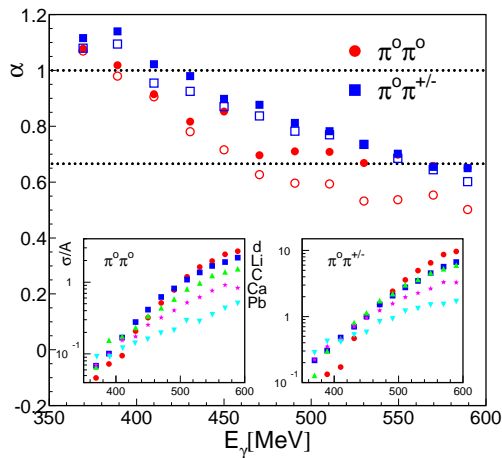


**Figure 14.** Scaling coefficient  $\alpha$  (see Eq. 1) for  $\pi^0\pi^0$  and  $\pi^0\pi^\pm$  production off nuclei as function of the incident photon energy. Filled symbols include the data from the deuteron, open symbols are from fits to Li, C, Ca, Pb data only. The inserts show for both reaction types the total cross sections in the threshold region normalized to the nuclear mass number  $A$ . The change from  $A$ -scaling close to threshold to  $A^{2/3}$  scaling at higher photon energies is clearly visible.

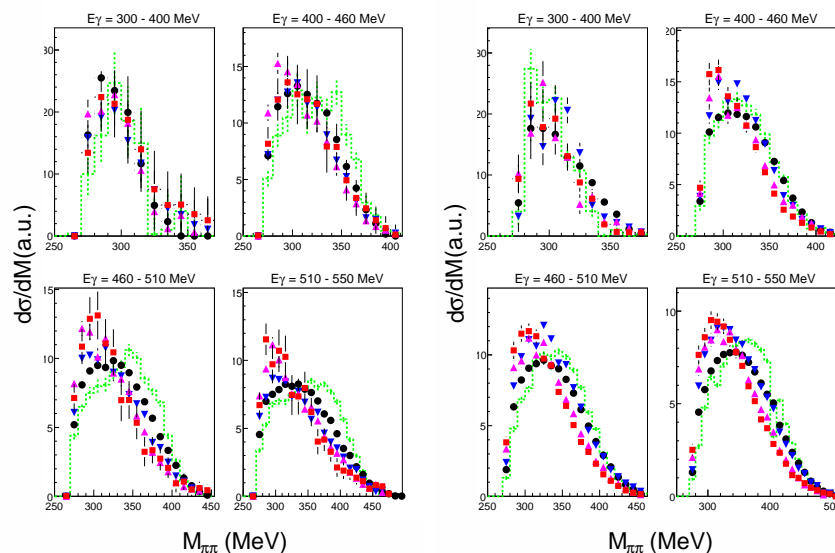


**Figure 15.** Preliminary invariant mass distributions of  $\pi^0\pi^0$  pairs (left hand side) and  $\pi^0\pi^\pm$  pairs (right hand side) off nuclei for different ranges of incident photon energy (all distributions normalized to total cross section). (Green) histograms: deuteron, (black) dots:  ${}^7\text{Li}$ , (blue) downward triangles:  ${}^{12}\text{C}$ , (magenta) upward triangles:  ${}^{40}\text{Ca}$ , (red) squares:  ${}^{nat}\text{Pb}$ .

#### 4. Conclusions

An overview was given on recent results from the photoproduction of mesons from nuclei. Quasi-free photoproduction from nucleons bound loosely in the deuteron has been established as a reliable tool for the study of the electromagnetic excitation spectrum of the neutron. The technical/instrumental challenges for the measurement of such reactions are well under control. Problems arising from nuclear effects like FSI can be very different depending on the studied reaction and must be carefully considered separately for each case. In particular for the examples of the  $\eta$  and  $\eta'$  mesons such problems seem to be negligible. Attempts to measure also (double) polarization observables for reactions off quasi-free neutrons with d-butanol targets are well under way and will in future largely contribute to the interpretation of the data in terms of nucleon resonance contributions. The most interesting current problem is certainly the not yet understood nature of the narrow structure in the excitation function for  $\eta$ -production off the neutron.

In view of  $\eta$ -mesic nuclei, the new data for  ${}^3\text{He}$  very convincingly confirm the unusual threshold behavior of coherent  $\eta$ -production off this nucleus, which completely disagrees with expectations from phase-space behavior and, together with the results from hadron induced reactions, points to the existence of a resonance overlapping with the production threshold.

The data for double pion production reactions off heavy nuclei confirm the earlier observed in-medium modifications of the invariant mass of the pion pairs, but suggest that the dominant effect is related to FSI rather than to in-medium modifications of the  $\sigma$ -meson.

### Acknowledgements

The results discussed in this paper have been obtained by the CBELSA/TAPS and Crystal Barrel/TAPS collaborations. They are part of the theses works of M. Dieterle, I. Jaegle, Y. Magrabi, F. Pheron, D. Werthmüller, and L. Witthauer. This work was supported by Schweizerischer Nationalfonds and Deutsche Forschungsgemeinschaft (SFB 443, SFB/TR-16.)

### References

- [1] Arndt R A *et al.* 2006 *Phys. Rev. C* **74** 045205
- [2] Nakamura K *et al.* 2010 *Journal of Physics G* **37** 075021
- [3] Edwards R G *et al.* 2011 *arXiv:[hep-ph]* **1104.5152**
- [4] Dürr S *et al.* 2008 *Science* **322** 1224
- [5] Bianchi N *et al.* 1996 *Phys. Rev. C* **54** 1688
- [6] Krusche B *et al.* 2002 *Phys. Lett. B* **526** 287
- [7] Krusche B 2005 *Eur. Phys. J. A* **26** 7
- [8] Tarbert C M *et al.* 2008 *Phys. Rev. Lett.* **100** 132301
- [9] Krusche B *et al.* 2004 *Eur. Phys. J. A* **22** 277
- [10] Röbig-Landau M *et al.* 1996 *Phys. Lett. B* **373** 45
- [11] Mertens T *et al.* 2008 *Eur. Phys. J. A* **38** 195
- [12] Nanova M *et al.* 2012 *submitted to Phys. Lett. B*
- [13] Trnka D *et al.* 2005 *Phys. Rev. Lett.* **94** 192303
- [14] Kotulla M *et al.* 2008 *Phys. Rev. Lett.* **100** 192302
- [15] Nanova M *et al.* 2010 *Phys. Rev. C* **82** 035209
- [16] Nanova M *et al.* 2011 *Eur. Phys. J. A* **47** 16
- [17] Ishikawa T *et al.* 2005 *Phys. Lett. B* **608** 215
- [18] Krusche B *et al.* 1997 *Phys. Lett. B* **397** 171
- [19] Liu L C and Haider Q 1986 *Phys. Rev. C* **34** 1845
- [20] Chrien R E *et al.* 1988 *Phys. Lett. B* **60** 2595
- [21] Johnson J D *et al.* 1993 *Phys. Rev. C* **47** 2571
- [22] Sokol G A *et al.* 1999 *Fizika B* **8** 85
- [23] Sokol G A and Pavlyuchenko L N 2008 *Phys. of. Atomic Nuclei* **71** 509
- [24] Arndt R A *et al.* 2005 *Phys. Rev. C* **72** 045202
- [25] Krusche B *et al.* 1995 *Phys. Rev. Lett.* **74** 3736
- [26] Krusche B *et al.* 1995 *Phys. Lett. B* **358** 40
- [27] Hoffmann-Rothe P *et al.* 1997 *Phys. Rev. Lett.* **78** 4697
- [28] Weiss J *et al.* 2001 *Eur. Phys. J. A* **11** 371
- [29] Weiss J *et al.* 2003 *Eur. Phys. J. A* **16** 275
- [30] Hejny V *et al.* 1999 *Eur. Phys. J. A* **6** 83
- [31] Hejny V *et al.* 2002 *Eur. Phys. J. A* **13** 493
- [32] Mersmann T *et al.* 2007 *Phys. Rev. Lett.* **98** 242301
- [33] Rausmann T *et al.* 2009 *Phys. Rev. C* **80** 017001
- [34] Pfeiffer M *et al.* 2004 *Phys. Rev. Lett.* **92** 252001
- [35] Bernard V, Meissner U G, Zahed I 1987 *Phys. Rev. Lett.* **59** 966
- [36] Hatsuda T, Kunihiro T and Shimizu H 1999 *Phys. Rev. Lett.* **82** 2840
- [37] Aouissat Z *et al.* 2000 *Phys. Rev. C* **61** 012201
- [38] Chiang H C, Oset E and Vicente Vacas M J 1998 *Nucl. Phys. A* **644** 77
- [39] Roca L, Oset E and Vicente Vacas M J 2002 *Phys. Lett. B* **541** 77
- [40] Bonutti F *et al.* 1996 *Phys. Rev. Lett.* **77** 603
- [41] Grion N *et al.* 2005 *Nucl. Phys. A* **763** 80
- [42] A. Starostin A *et al.* 2000 *Phys. Rev. Lett.* **85** 5539
- [43] Messchendorp J G *et al.* 2002 *Phys. Rev. Lett.* **89** 222302
- [44] Bloch F *et al.* 2007 *Eur. Phys. J. A* **32** 219
- [45] Krusche B 2011 *Eur. Phys. J. Special Topics* **198** 199
- [46] Husman D, Schuille W J 1988 *Phys. BL.* **44** 40

- [47] Hillert W 2006 *Eur. Phys. J. A* **28** 139
- [48] Jaegle I *et al.* 2011 *Eur. Phys. J. A* **47** 11
- [49] Jaegle I *et al.* 2011 *Eur. Phys. J. A* **47** 89
- [50] Aker E *et al.* 1992 *Nucl. Instr. and Meth. A* **321** 69
- [51] Novotny R 1991 *IEEE Trans. on Nucl. Science* **38** 379
- [52] Gabler A R *et al.* 1994 *Nucl. Instr. and Meth. A* **346** 168
- [53] Suft G *et al.* 2005 *Nucl. Inst. Meth. A* **538** 416
- [54] Herminghaus H *et al.* 1983 *IEEE Trans. on Nucl. Science.* **30** 3274
- [55] Kaiser K H *et al.* 2008 *Nucl. Inst. Meth. A* **593** 159
- [56] Anthony I *et al.* 1991 *Nucl. Inst. Meth. A* **301** 230
- [57] Starostin A *et al.* 2001 *Phys. Rev. C* **64** 055205
- [58] Watts D, in *Calorimetry in Particle Physics, Proceedings of the 11th International Conference, Perugia, Italy 2004*, edited by C. Cecchi, P. Cenci, P. Lubrano, and M. Pepe (World Scientific, Singapore, 2005, p. 560
- [59] Schumann S *et al.* 2010 *Eur. Phys. J. A* **43** 269
- [60] Zeitnitz C *et al.* 2001 *The GEANT-CALOR interface user's guide* (<http://www.staff.uni-mainz.de/zeitnitz/Gcalor/gcalor.html>)
- [61] Lacombe M *et al.* 1981 *Phys. Lett. B* **101** 139
- [62] Ajaka J *et al.* 1998 *Phys. Rev. Lett.* **81** 1797
- [63] Bock A *et al.* 1998 *Phys. Rev. Lett.* **81** 534
- [64] Armstrong C S *et al.* 1999 *Phys. Rev. D* **60** 052004
- [65] Thompson R *et al.* 2001 *Phys. Rev. Lett.* **86** 1702
- [66] Renard F *et al.* 2002 *Phys. Lett. B* **528** 215
- [67] Dugger M *et al.* 2002 *Phys. Rev. Lett.* **89** 222002
- [68] Crede V *et al.* 2005 *Phys. Rev. Lett.* **94** 012004
- [69] Nakabayashi T *et al.* 2006 *Phys. Rev. C* **74** 035202
- [70] Batalini O *et al.* 2007 *Eur. Phys. J. A* **33** 169
- [71] Bartholomy O *et al.* 2007 *Eur. Phys. J. A* **33** 133
- [72] Elsner D *et al.* 2007 *Eur. Phys. J. A* **33** 147
- [73] Denizli H *et al.* 2007 *Phys. Rev. C* **76** 015204
- [74] Williams M *et al.* 2009 *Phys. Rev. C* **80** 045213
- [75] Crede V *et al.* 2009 *Phys. Rev. C* **80** 055202
- [76] Sumihama M *et al.* 2009 *Phys. Rev. C* **80** 052201(R)
- [77] McNicoll E F *et al.* 2010 *Phys. Rev. C* **82** 035208
- [78] Chiang W T *et al.* 2002 *Nucl. Phys. A* **700** 429
- [79] Anisovich V A *et al.* 2005 *Eur. Phys. J. A* **25** 427
- [80] Krusche B and Schadmand S 2003 *Prog. Part. Nucl. Phys.* **51** 399
- [81] Moorehouse R G 1996 *Phys. Rev. Lett.* **16** 772
- [82] Kuznetsov V *et al.* 2007 *Phys. Lett. B* **647** 23
- [83] Miyahara F *et al.* 2007 *Prog. Theor. Phys. Suppl.* **168** 90
- [84] Jaegle I *et al.* 2007 *Phys. Rev. Lett.* **100** 252002
- [85] Shklyar V, Lenske H, Mosel U 2007 *Phys. Lett. B* **650** 172
- [86] Fix A, Tiator L, and Polyakov M V 2007 *Eur. Phys. J. A* **32** 311
- [87] Shyam R and Scholten O 2007 *Phys. Rev. C* **78** 065201
- [88] Anisovich V A *et al.* 2009 *Eur. Phys. J. A* **41** 13
- [89] Döring M and Nakayama K 2008 *Phys. Lett. B* **683** 145
- [90] Fantini A *et al.* 2008 *Phys. Rev. C* **78** 015203
- [91] Elsner D 2010 *Int. J. Mod. Phys. E* **19** 869
- [92] Plötzke R *et al.* 1998 *Phys. Lett. B* **444** 555
- [93] Dugger M *et al.* 2006 *Phys. Rev. Lett.* **96** 169905
- [94] Chiang W T *et al.* 2003 *Phys. Rev. C* **68** 045202
- [95] Nakayama K, Haberzettl H 2006 *Phys. Rev. C* **73** 045211
- [96] Drechsel D *et al.* 1999 *Nucl. Phys. A* **645** 145
- [97] Arndt R A *et al.* 2002 *Phys. Rev. C* **66** 055213
- [98] Krusche B *et al.* 1999 *Eur. Phys. J. A* **6** 309
- [99] Darwish E M, Arenhövel H, Schwamb M 2003 *Eur. Phys. J. A* **16** 111
- [100] Pheron F *et al.* 2012 *submitted to Phys. Lett. B*
- [101] Magrghi Y *et al.* 2012 *to be submitted to Phys. Lett. B*